Inorganic Chemistry Article

Inorg. Chem. **2010**, *49*, 4881–4894 **4881**
DOI: 10.1021/ic902467h

Crystallographic, Photophysical, NMR Spectroscopic and Reactivity Manifestations of the "8-Heteroaryl Effect" in 4,4-Difluoro-8-(C_4H_3X)-4-bora-3*a*,4*a*-diaza-*s*-indacene (X = O, S, Se) (BODIPY) Systems

Kibong Kim,[†] Changbum Jo,[†] Shanmugam Easwaramoorthi,[‡] Jooyoung Sung,[‡] Dong Ho Kim,[‡] and David G. Churchill*,[†]

[†]*Molecular Logic Gate Laboratory, Department of Chemistry, Korea Advanced Institute of Science and Technology (KAIST), 373-1 Guseong-dong, Yuseong-gu, Daejeon, 305-701, Republic of Korea, and* [‡]*Spectroscopy Laboratory for FPIES, Department of Chemistry, Yonsei University, Shinchon-dong 134, Seodaemoon-gu Seoul, 120-749, Republic of Korea*

Received December 12, 2009

We have synthesized and fully characterized three novel, yet closely related, heterocyclically *meso*-substituted (BODIPY) fluorophores 4,4-difluoro-8-(C_4H_3X)-4-bora-3*a*,4*a*-diaza-*s*-indacene (X=O, 2-/3-furyl (**7/10**); Se, 2-selenenyl (**9**)) through the use of 2-D NMR (COSY, HSQC, and HMBC), single crystal X-ray diffraction, mass spectrometry, elemental analysis, UV−vis spectroscopy, and fluorescent decay lifetimes, for comparison to the previously reported thienyl species (X = S, 2-/3-thienyl (**8/11**)). Specifically, **7**−**11** differ formally by chalcogen (O, S, or Se) or chalcogen placement. Solid state comparisons reveal major effects stemming from subtle structural differences which allows for insights into fluorescent crystal engineering. For the 2-heteroatom substitution, an increase in molecular weight (**7** < **8** < **9**) correlates with an increasing unit cell-volume, a greater orthogonality for the C_4H_3X group, and a lower value for Φ_F. Solution and density functional theory (DFT) results reveal interesting platforms for potential in fluorescent studies for neurology. 2-Heterocyclic species show larger $\lambda_{abs,max/em,max}$ values relative to 3-heterocyclic ones, based on electron withdrawing effects. **10** has the greatest Φ_F value herein (0.25, toluene). Fluorescence lifetimes were found to be 2.60 (**7**), 0.74 (**8**), 0.27 (**9**), 4.26 (**10**), and 1.86 ns (**11**); $\lambda_{em,max}$ decay was studied for **8**. Heterocyclic differences give rise to somewhat different pyrrolic NMR spectroscopic shifts as well. These compounds resist decomposition as seen from titrations with H_2O_2, and uniformly undergo $\lambda_{abs,max}$ red-shifting and lowered Φ_F values as they become brominated with Br_2.

1. Introduction

The use of fluorescent dyes in the biosciences has led to the emergence and development of numerous families of derivatized compounds in an effort to find substrates with optimal photophysical tuning, often for bioconjugation, in the probing of important in vivo processes.[1−4] In terms of the tuning of optical properties, there are various ways to substitute any fluorogenic framework so to significantly alter, or enhance, its properties.[5] Further, these derivatized probes must be robust, potentially to withstand harsh oxidative conditions. Molecular probes in, for example, the neurosciences depend on their ability to report inter- or intracellular concentrations under strong oxidative conditions, as the brain is rich with chemical oxidation events.[6−8] Such probes that need to pass through the blood brain barrier, require various properties. Importantly, it is currently understood that the molecular size for blood brain barrier crossing must be small (< ∼500 Da).[9,10,11a] If we follow the argument of size, more compact ways to impart fluorophore substitutive effects is required. One compactness strategy is to impart endocyclic substitution, versus exocylic substituents;

*To whom correspondence should be addressed. E-mail: dchurchill@kaist.ac.kr. Fax: +82-42-350-2810.

(1) de Silva, A. P.; Fox, D. B.; Huxley, A. J. M.; Moody, T. S. *Coord. Chem. Rev.* **2000**, *205*, 41.
(2) Amendola, V.; Fabbrizzi, L.; Foti, F.; Licchelli, M.; Mangano, C.; Pallavicini, P.; Poggi, A.; Sacchi, D.; Taglietti, A. *Coord. Chem. Rev.* **2006**, *250*, 273.
(3) Valeur, B.; Leray, I. *Coord. Chem. Rev.* **2000**, *205*, 3.
(4) de Silva, A. P.; Gunaratne, H. Q. N.; Gunnlaugsson, T.; Huxley, A. J. M.; McCoy, C. P.; Rademacher, J. T.; Rice, T. E. *Chem. Rev.* **1997**, *97*, 1515.
(5) Kee, H. L.; Kirmaier, C.; Yu, L. H.; Thamyongkit, P.; Youngblood, W. J.; Calder, M. E.; Ramos, L.; Noll, B. C.; Bocian, D. F.; Scheidt, W. R.; Birge, R. R.; Lindsey, J. S.; Holten, D. *J. Phys. Chem. B* **2005**, *109*, 20433.
(6) Bao, L.; Avshalumov, M. V.; Patel, J. C.; Lee, C. R.; Miller, E. W.; Chang, C. J.; Rice, M. E. *J. Neurosci.* **2009**, *29*, 9002.
(7) Srikun, D.; Miller, E. W.; Domaille, D. W.; Chang, C. J. *J. Am. Chem. Soc.* **2008**, *130*, 4596.
(8) Dickinson, B. C.; Chang, C. J. *J. Am. Chem. Soc.* **2008**, *130*, 9638.
(9) Gaeta, A.; Hider, R. C. *Br. J. Pharmacol.* **2005**, *146*, 1041.
(10) Liu, Z. D.; Hider, R. C. *Coord. Chem. Rev.* **2002**, *232*, 151.
(11) (a) Habgood, M. D.; ZuDong, L.; Dehkordi, L.; Nazarian, J.; Abraham, M.; Hider, R. C.; Abbott, N. J. *J. Physiol.* **1997**, *505P*, 49P. (b) Chang, E.; Honson, N. S.; Bandyopadhyay, B.; Funk, K. E.; Jensen, J. R.; Kim, S.; Naphade, S.; Kuret, J. *Curr. Alzheimer Res.* **2009**, *6*, 409–414.

© 2010 American Chemical Society

that is, in place of a benzene ring, there can be convenient formal addition of a thienyl (SC_4H_3), furyl (OC_4H_3) or selenyl (SeC_4H_3) group. A detailed comparison of such closely related species is interesting, not only optically (in solution), but also in the solid state (crystallographically). Further, how dye molecules stack, as well as their inherent design, may also be of interest in anti-aggregation inhibitors for various disease-related proteins.[11b] Importantly, one-atom changes will alter slightly crystallographic parameters and packing considerations of the dye dense solids. Species that differ by a chalcogen atom (O, S, Se) allow for decisive site-specific alterations in fluorophore chemistry. For instance, an ethereal sulfur could oxidize to the sulfone, whereas oxygen does not permit such hypervalence. There are previous reports relating to interesting chalcogen-containing molecules of one-atom difference.[12,13] However, most of these describe structural properties. In reports by Parkin and co-workers, chalcogen atoms located in various systems indicate how such subtle formal "tweaking" may affect reactivity, for example, in the bridge of zirconium and hafnium compounds,[14−18] or as terminal chalcogenides in tungsten and molybdenum compounds.[19−22] In one aspect of our research, we are currently driven by the desire to make better Tau protein antiaggregation probes or binding molecules which deals with a balance between fluorescence and lipophilicity (and charge), not to mention a consideration of pharmacokinetics; the precursors could be modified and screened in this context at a later time.[23]

It is not an overstatement to say that BODIPY research has experienced an explosion of interest in recent years. BODIPY is by now a very well-known fluorophore system; and there are a variety of substituted species and conjugations, as well as multimeric designs and BODIPY analogues (e.g., crown-ether- and porphyrin-conjugated, and polymeric frameworks).[24,25] They are quite easy to synthesize from, for example, their corresponding aldehyde (with pyrrole) with subsequent treatment with $BF_3 \cdot OEt_2$, and are intriguing in the way that their optical properties or specific interaction with external stimulants are not readily predictable. Recently, many researchers have reported BODIPY fluorophores in the context of molecular sensing, molecular logic gating, cellular imaging, and so forth.[25−33] Of all possible conjugations, 8-position substitution continues to be well-explored and to reap unexpected results in molecular recognition. In terms of basic research, it was clarified in 2005 that subtle 8-position BODIPY substitution can dramatically change the fluorophore's optical properties.[5] Even though many BODIPY systems bearing various substituents,[34] including thiophene motifs[35] have been reported, there were no reports on discrete 8-substituted 5-membered ring substitution prior to our studies;[32,36,37a,38] There was, however, a report of BODIPY functionalized oligothiophene sequences made by Andrioletti, Clays, and co-workers in 2008.[37b] Nonetheless, there have been no reports focusing on differences in the context of one-atom congeneric (e.g., chalcogen) differences in 8-position substitution, to the best of our knowledge either. Thus, herein, we are focusing on the core 8-aryl substituted BODIPY-type systems bearing closely related ring differences: 4,4-difluoro-8-(C_4H_3X)-4-bora-3*a*,4*a*-diaza-*s*-indacene (X = O, 2-/3-furyl (**7**/**10**); Se, 2-selenenyl (**9**)) for comparison to the previously reported (X = S, 2-, (**8**) and 3-thienyl, (**11**)) species. In terms of nomenclature, the novel compounds herein can also be considered as *N*,*N*-difluoroboryl-5-(*Ar*)dipyrrins (*Ar* = 2-furyl, **7**; 2-selenenyl, **9**; 3-furyl, **10**). We can characterize these systems by a variety of spectroscopic techniques. Since the fluorescence quantum yield (Φ_F) is quite high for BODIPY, their excited state lifetimes can be obtained and compared. Further, we can consider how solid state and reactivity differences weigh into a full consideration of these closely related geometries.

2. Experimental Section

General Considerations. All chemicals used herein were used as received from commercial suppliers (Aldrich, Acros, and Junsei companies). 2-Selenophene carboxaldehyde is synthesized by the well-known Vilsmeier−Haack reaction.[39] The synthetic details for the preparation of the dipyrromethanes and for the BODIPY systems follow literature methods.[40−42] Compounds **3**, **6**, **8**, and **11** have been previously reported by this research group.[37,38] ^{1}H and ^{13}C NMR spectra were acquired using a Bruker Avance 300 or 400 MHz spectrometer. TMS was used as an internal standard. ^{1}H and ^{13}C NMR spectral signals were calibrated internally by the respective protio impurity or

(12) Evans, W. J.; Rabe, G. W.; Ziller, J. W.; Doedens, R. J. *Inorg. Chem.* **1994**, *33*, 2719.
(13) Cummins, C. C.; Schrock, R. R.; Davis, W. M. *Inorg. Chem.* **1994**, *33*, 1448.
(14) Howard, W. A.; Parkin, G. *J. Organomet. Chem.* **1994**, *472*, C1.
(15) Howard, W. A.; Parkin, G. *J. Am. Chem. Soc.* **1994**, *116*, 606.
(16) Howard, W. A.; Trnka, T. M.; Parkin, G. *Inorg. Chem.* **1995**, *34*, 5900.
(17) Howard, W. A.; Trnka, T. M.; Waters, M.; Parkin, G. *J. Organomet. Chem.* **1997**, *528*, 95.
(18) Shin, J. H.; Hascall, T.; Parkin, G. *Organometallics* **1999**, *18*, 6.
(19) Murphy, V. J.; Parkin, G. *J. Am. Chem. Soc.* **1995**, *117*, 3522.
(20) Shin, J. H.; Churchill, D. G.; Bridgewater, B. M.; Pang, K. L.; Parkin, G. *Inorg. Chim. Acta* **2006**, *359*, 2942.
(21) Shin, J. H.; Savage, W.; Murphy, V. J.; Bonanno, J. B.; Churchill, D. G.; Parkin, G. *J. Chem. Soc., Dalton Trans.* **2001**, 1732.
(22) Rabinovich, D.; Parkin, G. *Inorg. Chem.* **1995**, *34*, 6341.
(23) Nakai, J.; Ohkura, M.; Imoto, K. *Nat. Biotechnol.* **2001**, *19*, 137.
(24) Loudet, A.; Burgess, K. *Chem. Rev.* **2007**, *107*, 4891.
(25) Yuan, M. J.; Li, Y. L.; Li, J. B.; Li, C. H.; Liu, X. F.; Lv, J.; Xu, J. L.; Liu, H. B.; Wang, S.; Zhu, D. *Org. Lett.* **2007**, *9*, 2313.
(26) Ojida, A.; Sakamoto, T.; Inoue, M.; Fujishima, S.; Lippens, G.; Hamachi, I. *J. Am. Chem. Soc.* **2009**, *131*, 6543.
(27) Atilgan, S.; Ozdemir, T.; Akkaya, E. U. *Org. Lett.* **2008**, *10*, 4065.
(28) Yuan, M. J.; Zhou, W. D.; Liu, X. F.; Zhu, M.; Li, J. B.; Yin, X. D.; Zheng, H. Y.; Zuo, Z. C.; Ouyang, C.; Liu, H. B.; Li, Y. L.; Zhu, D. B. *J. Org. Chem.* **2008**, *73*, 5008.
(29) Ekmekci, Z.; Yilmaz, M. D.; Akkaya, E. U. *Org. Lett.* **2008**, *10*, 461.
(30) Cheng, T. Y.; Xu, Y. F.; Zhang, S. Y.; Zhu, W. P.; Qian, X. H.; Duan, L. P. *J. Am. Chem. Soc.* **2008**, *130*, 16160.
(31) Peng, X. J.; Du, J. J.; Fan, J. L.; Wang, J. Y.; Wu, Y. K.; Zhao, J. Z.; Sun, S. G.; Xu, T. *J. Am. Chem. Soc.* **2007**, *129*, 1500.
(32) Choi, S. H.; Pang, K.; Kim, K.; Churchill, D. G. *Inorg. Chem.* **2007**, *46*, 10564.
(33) Rohr, H.; Trieflinger, C.; Rurack, K.; Daub, J. *Chem.—Eur. J.* **2006**, *12*, 689.
(34) Fron, E.; Coutino-Gonzalez, E.; Pandey, L.; Sliwa, M.; Van der Auweraer, M.; De Schryver, F. C.; Thomas, J.; Dong, Z. Y.; Leen, V.; Smet, M.; Dehaen, W.; Vosch, T. *New J. Chem.* **2009**, *33*, 1490.
(35) (a) Rihn, S.; Retailleau, P.; Bugsaliewicz, N.; De Nicola, A.; Ziessel, R. *Tetrahedron Lett.* **2009**, *50*, 7008. (b) Haugland, R. P.; Kang, H. C. (Molecular Probes, Inc., U.S.A.). U.S. Patent 5,248,782, **1993**.
(36) Choi, S. H.; Kim, K.; Jeon, J.; Meka, B.; Bucella, D.; Pang, K.; Khatua, S.; Lee, J.; Churchill, D. G. *Inorg. Chem.* **2008**, *47*, 11071.
(37) (a) Choi, S. H.; Kim, K.; Lee, J.; Do, Y.; Churchill, D. G. *J. Chem. Crystallogr.* **2007**, *37*, 315. (b) Zrig, S.; Remy, P.; Andrioletti, B.; Rose, E.; Asselberghs, I.; Clays, K. *J. Org. Chem.* **2008**, *73*, 1563–1566.
(38) Maiti, N.; Lee, J.; Do, Y.; Shin, H. S.; Churchill, D. G. *J. Chem. Crystallogr.* **2005**, *35*, 949.
(39) Arena, G.; Cali, R.; Maccarone, E.; Passerini, A. *J. Chem. Soc., Perkin Trans. 2* **1993**, 1941.
(40) Brückner, C.; Karunaratne, V.; Rettig, S. J.; Dolphin, D. *Can. J. Chem.* **1996**, *74*, 2182.
(41) Wagner, R. W.; Lindsey, J. S. *Pure Appl. Chem.* **1996**, *68*, 1373.
(42) Lee, C. H.; Lindsey, J. S. *Tetrahedron* **1994**, *50*, 11427.

carbon resonance of the $CDCl_3$ (^{1}H: δ 7.24; ^{13}C: δ 77.0) or CD_2Cl_2 solvent (^{1}H: δ 5.32, ^{13}C: δ 53.8). C, H, N elemental analyses were measured using a Vario EL III CHNS elemental analyzer. High resolution matrix-assisted laser desorption/ionization (MALDI) mass spectrometry was performed on a VG AUTOSPEC ULTIMA by the research support staff at KAIST. This instrument possesses a trisector double focusing magnetic sector analyzer and was operated at a resolution of 80,000.

Preparation of 2-Selenophenecarboxaldehyde[39] **(1).** Selenophene (2.5 g, 19 mmol) was dissolved in *N*,*N*-dimethylformamide (DMF, 2.0 mL, 25.8 mmol), then phosphoryl chloride (2.40 mL, 25.7 mmol) was added. After a period of 30 min under N_2 at 65 °C during which the reaction was allowed to proceed, the reaction mixture was then poured into an ice bath. Then, sodium acetate (~35 g) was added. After extraction with diethyl ether (×3), the mixture was dried under anhydrous magnesium sulfate. The solvent was removed under rotary evaporation, and a yellow oil is obtained. Yield: 2.07 g (68.0%), ^{1}H NMR ($CDCl_3$, δ 7.24): δ 9.78 (s, 1H), 8.00 (d, 1H), 7.45 (m, 1H), 8.49 (d, 1H).

General Procedure for the Synthesis of Dipyrromethane Reported Herein. Aldehyde (1.0 equiv) and pyrrole (25 equiv) were added into a two-neck flask; sparging with N_2 for 10 min was then undertaken to remove atmospheric oxygen. Trifluoroacetic acid (TFA, 0.1 equiv) is added dropwise. After ~1 h of allowing these materials to react under N_2, triethylamine was added to maintain a pH of ~7. The reaction mixture was then diluted with ethyl acetate, and washed with distilled water (×3). The organic layer was then collected and dried over anhydrous magnesium sulfate. Under rotary evaporation, solvent was removed, and a brown oil is obtained. Silica gel column chromatography with eluent (dichloromethane/hexane = 1:2) followed by rotary evaporation afforded a light yellow solid.

Synthesis of 5(2-Furyl)dipyrromethane (2). 2-Furylcarboxaldehyde (2.5 mL, 30 mmol), pyrrole (52 mL, 750 mmol), and TFA (0.22 mL, 3.0 mmol) were used in accordance with the general procedure above. Yield: 3.81 g (59.8%). ^{1}H NMR (CD_2Cl_2, δ 5.32): δ 8.20 (br, 2H), 7.42 (s, 1H), 6.69 (s, 2H), 6.36 (s, 1H), 6.16 (s, 1H), 6.12 (m, 2H), 5.96 (s, 2H), 5.51 (s, 1H).

Synthesis of 5(2-Selenenyl)dipyrromethane (4). 2-Selenophenecarboxaldehyde (2.00 g, 12.9 mmol), pyrrole (22.4 mL, 323 mmol), and trifluoroacetic acid (TFA, 0.10 mL, 1.3 mmol) were used in accordance with the general procedure above. Yield: 1.36 g (38.2%). ^{1}H NMR (CD_2Cl_2, δ 5.32): δ 8.10 (br, 2H), 7.91 (m, 1H), 7.15 (m, 1H), 7.05 (d, 1H), 6.75 (m, 2H), 6.15 (m, 2H), 6.10 (s, 2H), 5.75 (s, 1H).

Synthesis of 5(3-Furyl)dipyrromethane (5). 3-Furylcarboxaldehyde (2.5 mL, 30 mmol), pyrrole (52.0 mL, 750 mmol), and TFA (0.22 mL, 3.0 mmol) were used in accordance with the general procedure above. Yield: 3.05 g (47.9%). ^{1}H NMR (CD_2Cl_2, δ 5.32): δ 8.02 (br, 2H), 7.42 (m, 1H), 7.24 (m, 1H), 6.67 (m, 2H), 6.34 (s, 1H), 6.12 (m, 2H), 5.97 (m, 2H), 5.36 (s, 1H).

General Procedure of Synthesis of BODIPY. A sample of dipyrromethane is dissolved in anhydrous tetrahydrofuran (THF), and DDQ (2,3-dichloro-5,6-dicyano-*p*-benzoquinone) in anhydrous THF is added slowly. After stirring at room temperature (3 h), triethylamine is added, followed by 10 min of additional stirring. Boron trifluoride etherate is then added, and the reaction flask is heated to reflux for 16 h. A thin-layer chromatography (TLC) assay revealed the expected dominant orange-red spot at R_f = ~ 0.3−0.4 (MC/Hx 1:1). The reaction mixture was then diluted with dichloromethane before being filtered through a silica gel pad. The volume of solvent was then reduced, so to concentrate the eluent; this condensate is then washed with distilled water (×3). The organic layer is collected and dried over anhydrous magnesium sulfate. Silica gel column chromatography with eluent (dichloromethane: hexane = 1: 2) gives the expected BODIPY product. Single crystals suitable for X-ray diffraction study were obtained from a solvent system composed of dichloromethane and hexane.

Synthesis of 4,4-Difluoro-8-(2-furyl)-4-bora-3*a*,4*a*-diaza-*s*-indacene or Difluoroboryl-5(2-furyl)dipyrrin (7). 5(2-furyl)dipyrromethane (1.00 g, 4.71 mmol), DDQ (1.17 g, 5.18 mmol), triethylamine (3.3 mL, 23.7 mmol), and boron trifluoride diethyrate (3.0 mL, 24 mmol) were used in accordance with the general procedure given above. Yield: 4.4%. ^{1}H NMR ($CDCl_3$, δ 7.24): δ 7.86 (s, $2H_1$), 7.80 (d, $^3J_{H-H}$ = 1.4 Hz, $1H_9$), 7.44 (d, $^3J_{H-H}$ = 4.2 Hz, $2H_3$), 7.17 (d, $^3J_{H-H}$ = 3.6 Hz, $1H_7$), 6.68 (dd, $^3J_{H-H}$ = 3.5 Hz, $^3J_{H-H}$ = 1.8 Hz, $1H_8$), 6.56 (d, $^3J_{H-H}$ = 4.0 Hz, $2H_2$). ^{13}C NMR ($CDCl_3$, δ 77.0): 148.6 (C_6), 147.8 (ddd, $^1J_{C-H}$ = 203.9 Hz, $^2J_{C-H}$ = 10.7 Hz, $^3J_{C-H}$ = 7.8 Hz, C_9), 143.0 (dt, $^1J_{C-H}$ = 184.9 Hz, $^3J_{C-F}$ = 9.0 Hz, C_1), 132.8 (C_5), 132.2 (C_4), 130.6 (d, $^1J_{C-H}$ = 175.5 Hz, C_3), 120.6 (ddd, $^1J_{C-H}$ = 176.8 Hz, $^2J_{C-H}$ = 5.5 Hz, $^3J_{C-H}$ = 4.3 Hz, C_7), 118.3 (d, $^1J_{C-H}$ = 176.3 Hz, C_2), 113.4 (ddd, $^1J_{C-H}$ = 177.4 Hz, $^2J_{C-H}$ = 12.6 Hz, $^3J_{C-H}$ = 3.3 Hz, C_8). MALDI-TOF: $(M - F)^+$ 239.150 (*m*/*z*) (Calculated: 239.079). ^{11}B-NMR ($CDCl_3$, $BF_3 \cdot OEt_2$, δ 0.00): δ 0.20 (t, $^1J_{B-F}$ = 28.5 Hz). ^{19}F-NMR ($CDCl_3$): δ 146.26 (q, $^1J_{B-F}$ = 28.5 Hz). Anal. Calcd for $C_{13}H_9BF_2N_2O$: C 60.51, H 3.52, N 10.86, found: C 60.42, H 4.03, N 10.27.

Synthesis of 4,4-Difluoro-8-(2-selenenyl)-4-bora-3*a*,4*a*-diaza-*s*-indacene or Difluoroboryl-5-(2-selenenyl)dipyrrin (9). 5(2-selenenyl)dipyrromethane (1.00 g, 3.62 mmol), DDQ (0.90 g, 3.98 mmol), triethylamine (5.05 mL, 36.0 mmol), and boron trifluoride diethyrate (4.60 mL, 36.0 mmol) were used in accordance with the general procedure given above. Yield: 9.4%. ^{1}H NMR ($CDCl_3$, δ 7.24): δ 8.40 (d, $^3J_{H-H}$ = 5.5 Hz, $1H_9$), 7.91 (s, $2H_1$), 7.71 (d, $^3J_{H-H}$ = 3.8 Hz, $1H_7$), 7.49 (dd, $^3J_{H-H}$ = 5.5 Hz, $^3J_{H-H}$ = 3.9 Hz, $1H_8$), 7.24 (d, $^3J_{H-H}$ = 3.3 Hz, $2H_3$), 6.55 (d, $^3J_{H-H}$ = 4.0 Hz, $2H_2$). ^{13}C NMR ($CDCl_3$, δ 77.0): δ 143.8 (dt, $^1J_{C-H}$ = 184.8 Hz, $^3J_{C-F}$ = 9.0 Hz, C_1), 141.7 (C_5), 139.1 (C_6), 137.7 (ddd, $^1J_{C-H}$ = 187.4 Hz, $^2J_{C-H}$ = 10.9 Hz, $^3J_{C-H}$ = 6.3 Hz, C_9), 134.9 (ddd, $^1J_{C-H}$ = 165.6 Hz, $^2J_{C-H}$ = 10.0 Hz, $^3J_{C-H}$ = 6.9 Hz, C_7), 134.2 (C_4), 131.5 (d, $^1J_{C-H}$ = 172.8 Hz, C_3), 130.5 (ddd, $^1J_{C-H}$ = 165.9 Hz, $^2J_{C-H}$ = 6.3 Hz, $^3J_{C-H}$ = 3.9 Hz, C_8), 118.4 (d, $^1J_{C-H}$ = 177.8 Hz, C_2). MALDI-TOF: $(M - F)^+$ 303.148 (*m*/*z*) (Calculated: 303.001). ^{11}B-NMR ($CDCl_3$, $BF_3 \cdot OEt_2$, δ 0.00): δ 0.23 (t, $^1J_{B-F}$ = 28.6 Hz). ^{19}F-NMR ($CDCl_3$): δ 145.78 (q, $^1J_{B-F}$ = 28.8 Hz). Anal. Calcd for $C_{13}H_9BF_2N_2Se$: C 48.64, H 2.83, N 8.73, found: C 47.30, H 3.15, N 8.33.

Synthesis of 4,4-Difluoro-8-(3-furyl)-4-bora-3*a*,4*a*-diaza-*s*-indacene or Difluoroboryl-5-(3-furyl)dipyrrin (10). 5(3-furyl)dipyrromethane (1.50 g, 7.07 mmol), DDQ (1.90 g, 8.40 mmol), triethylamine (10.6 mL, 76.0 mmol), and boron trifluoride diethyrate (8.90 mL, 71.0 mmol) were used in accordance with the general procedure given above. Yield: 21.5%, ^{1}H NMR ($CDCl_3$, δ 7.24): δ 7.89 (s, $2H_1$), 7.83 (s, $1H_9$), 7.61 (dd, $^3J_{H-H}$ = ~2 Hz, $^3J_{H-H}$ = ~2 Hz $1H_8$), 7.18 (d, $^3J_{H-H}$ = 4.2 Hz, $2H_3$), 6.75 (m (an expected dd), $1H_7$), 6.54 (d, $^3J_{H-H}$ = 3.9 Hz, $2H_2$). ^{13}C NMR ($CDCl_3$, δ 77.0): δ 144.7 (dt, $^1J_{C-H}$ = 204.9 Hz, $^2J_{C-H}$ = 6.3 Hz, C_9), 144.3 (ddd, $^1J_{C-H}$ = 204.5 Hz, $^2J_{C-H}$ = 10.2 Hz, $^3J_{C-H}$ = 7.0 Hz, C_8), 143.8 (dt, $^1J_{C-H}$ = 184.9 Hz, $^3J_{C-F}$ = 8.8 Hz, C_1), 138.4 (C_5), 134.2 (C_4), 130.2 (d, $^1J_{C-H}$ = 175.0 Hz, C_3), 119.9 (C_6), 118.3 (d, $^1J_{C-H}$ = 173.2 Hz, C_2), 112.5 (ddd, $^1J_{C-H}$ = 177.3 Hz, $^2J_{C-H}$ = 13.3 Hz, $^3J_{C-H}$ = 4.6 Hz, C_7). MALDI-TOF: $(M - F)^+$ 239.144 (*m*/*z*) (Calculated: 239.079). ^{11}B-NMR ($CDCl_3$, $BF_3 \cdot OEt_2$, δ 0.00): δ 0.24 (t, $^1J_{B-F}$ = 28.7 Hz). ^{19}F-NMR ($CDCl_3$): δ 145.89 (q, $^1J_{B-F}$ = 28.79 Hz). Anal. Calcd for $C_{13}H_9BF_2N_2O$: C 60.51, H 3.52, N 10.86, found: C 61.09, H 3.68, N 11.26.

Absorption and Emission spectroscopy. All compounds were dissolved in various solvents to acquire optical measurements. Acetonitrile, toluene, methanol, and dichloromethane were all individually used in preparing a BODIPY solution of concentration 5.0×10^{-6} M. UV−vis absorption and emission measurements are obtained using a CARY 300 Bio UV−vis spectrometer and a Shimatzu RF-5301 PC spectrophotometer, respectively. Emission spectra are obtained through the excitation of λ_{max} from the absorption spectrum of each compound.

Scheme 1. Synthetic Scheme of BODIPY Molecules (**7**−**11**)

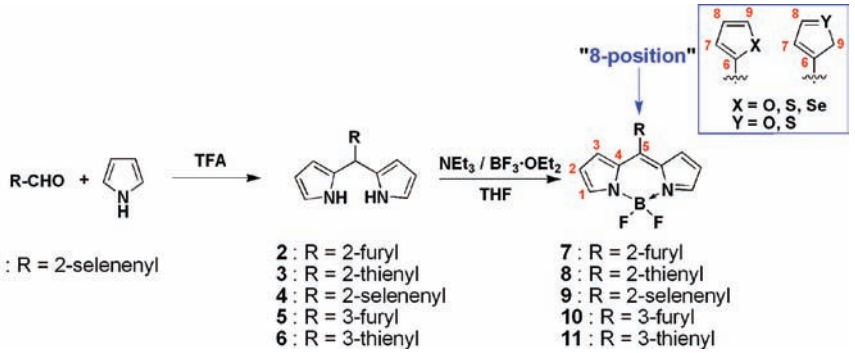

Fluorescein in 0.1 N NaOH ($\Phi_F = 0.92$)[43] is used as the standard to calibrate the quantum yield. For the titration study, hydrogen peroxide and molecular bromine (Br_2) are dissolved in acetonitrile and carefully titrated by syringe to the BODIPY solution at room temperature.

X-ray Crystallography Details. X-ray diffraction measurements were performed at ∼300 K (for **7**) and ∼100 K (for **9**, **10**) with a Bruker SMART 1K CCD diffractometer using graphite-monochromated Mo-Kα radiation (λ = 0.71073 Å). Cell parameters were determined and refined through the use of the SMART program.[44] Data reduction was performed using SAINT software.[44] The data were corrected for Lorentz and polarization effects. An empirical absorption correction was applied using the SADABS program.[45] All intensity data were corrected for Lorentz and polarization effects. The crystallographic molecular structures were solved by direct methods using the SHELXS-97 program[46] and were refined by full matrix least-squares calculations (F^2) through the use of SHELXL-97 software.[47] All non-H atoms were refined anisotropically against F^2 for all reflections. All hydrogen atoms were placed at their calculated positions and refined isotropically. Crystal data for compounds **7**, **9**, and **10** and selected bond lengths and angles are listed in the Supporting Information. The *.cif files were deposited with the Cambridge Crystallographic Data Centre and the following codes were allocated: CCDC-756065 (**7**), CCDC-756066 (**9**), and CCDC-756067 (**10**). These data can be obtained free of charge via the Internet: www.ccdc.cam.ac.uk/data_request/cif.

Computational Details. All geometries were optimized by way of density functional theory (DFT) methods using the combined Becke's three parameter exchange functional and the gradient-corrected correlation functional of Lee, Yang, and Parr, known as the B3LYP method,[48,49] in conjunction with the standard 6-31G(d,p) basis set except for the selenium atom (cc-pVTZ). Calculations were performed with the Gaussian 03 suite of programs.[50] Molecular orbitals and highest occupied molecular orbital (HOMO)−lowest unoccupied molecular orbital (LUMO) levels for several geometries were also generated and prepared graphically with this software. Input geometries were readily derived from related X-ray coordinates; and geometry optimization was performed without any imposed geometrical constraints. Vibrational frequencies were also calculated for all unconstrained geometry optimization structures; imaginary frequencies were absent in all such optimized structures, signifying true minima. Relative electronic energies for the calculated species are provided (in kcal mol^{-1}), albeit for the gas phase, for comparison in the manuscript text.

3. Results and Discussion

Synthesis and NMR Characterization. BODIPY systems (**7**−**11**) are synthesized in a quite straightforward way from commercially available aldehyde precursors. (Scheme 1) Only 2-selenophene carboxaldehyde was synthesized via the Vilsmeier−Haack reaction from selenophene and phosphoryl chloride.[39] Dipyrromethane is formed from aldehyde and pyrrole[42] and can oxidize with DDQ[40] with addition of triethylamine and boron trifluoride dietherate[41] to give the expected bright red-orange product(s). By TLC plate assaying, the product spot shows the characteristic brilliant orange spot under white light and a yellow fluorescent spot under UV light (benchtop lamp, λ_{ex} = 365 nm). The crude reaction mixture was then washed with water and passed down a silica gel chromatographic column so to afford a dark orange solid upon rotary evaporation and after further drying. Recrystallization from dichloromethane and hexane gives jewel-like single crystals, many of which are suitable for an X-ray diffraction study. Difluoroboryl-(3-selenenyl)dipyrrin was not synthesized as of yet because of difficulties in preparing 3-selenenylcarboxaldehyde.

Various solution NMR spectroscopic techniques were used to satisfactorily characterize compounds **7**, **9**, and **10**. Specifically, all proton and carbon resonances present in the spectra were unambiguously assigned to the atoms of the dye molecules. A variety of NMR experiments were used: All reproductions of ^{1}H, ^{13}C, ^{13}C{^{1}H coupled} NMR

(43) Demas, J. N. In *Optical Radiation Measurements*; Mielenz, K. D., Ed.; Academic Press: New York, 1982; Vol. *3* (Measurement of Photoluminescence), pp 195−248.
(44) *SMART and SAINT*, Area Detector Software Package and SAX Area Detector Integration Program; Bruker Analytical X-ray: Madison, WI, 1997.
(45) *SADABS*, Area Detector Absorption Correction Program; Bruker Analytical X-ray: Madison, WI, 1997.
(46) Sheldrick, G. M. SHELXS-97, Program for Crystal Structure Determination. *Acta Crystallogr*. **1990**, *A46*, 467−473.
(47) (a) Sheldrick, G. M. *SHELXL-97*, Program for Crystal Structure Solution and Refinements; Universität Göttingen: Göttingen, Germany, 1999. (b) Sheldrick, G. M. *Acta Crystallogr*. **2008**, *A64*, 112–122.
(48) Becke, A. D. *J. Chem. Phys*. **1993**, *98*, 5648.
(49) Lee, C. T.; Yang, W. T.; Parr, R. G. *Phys. Rev. B* **1988**, *37*, 785.
(50) Frisch, M. J.; Trucks, G. W.; Schlegel, H. B.; Scuseria, G. E.; Robb, M.; Cheeseman, J. R.; Montgomery, J. A.; Vreven, J. A.; Kudin, K. N.; Burant, J. C.; Millam, J. M.; Iyengar, S. S.; Tomasi, J.; Barone, V.; Mennucci, B.; Cossi, M.; Scalmani, G.; Rega, N.; Petersson, G. A.; Nakatsuji, H.; Hada, M.; Ehara, M.; Toyota, K. ; Fukuda, R.; Hasegawa, J.; Ishida, M.; Nakajima, T.; Honda, Y.; Kitao, O.; Nakai, H.; Klene, M.; Li, X.; Knox, J. E.; Hratchian, H. P.; Cross, J. B.; Adamo, C.; Jaramillo, J; Gomperts, R.; Stratmann, R. E.; Yazyev, O.; Austin, A. J.; Cammi, R.; Pomelli, C.; Ochterski, J. W.; Ayala, P. Y.; Morokuma, K.; Voth, G. A.; Salvador, P.; Dannenberg, J. J.; Zakrzewski, V. G.; Dapprich, S.; Daniels, A. D.; Strain, M. C.; Farkas, O.; Malick, D. K.; Rabuck, A. D.; Raghavachari, K.; Foresman, J. B.; Ortiz, J. V.; Cui, Q. ; Baboul, A. G. ; Clifford, S. ; Cioslowski, J.; Stefanov, B. B.; Liu, G.; Liashenko, A.; Piskorz, P.; Komaromi, I.; Martin, R. L.; Fox, D. J.; Keith, T.; Al-Laham, M. A.; Peng, C. Y.; Nanayakkara, A.; Challacombe, M.; Gill, P. M. W.; Johnson, B.; Chen, W.; Wong, M. W.; Gonzalez, C.; Pople, J. A. *Gaussian 03*, Revision A.1; Gaussian, Inc.: Pittsburgh, PA, 2003.

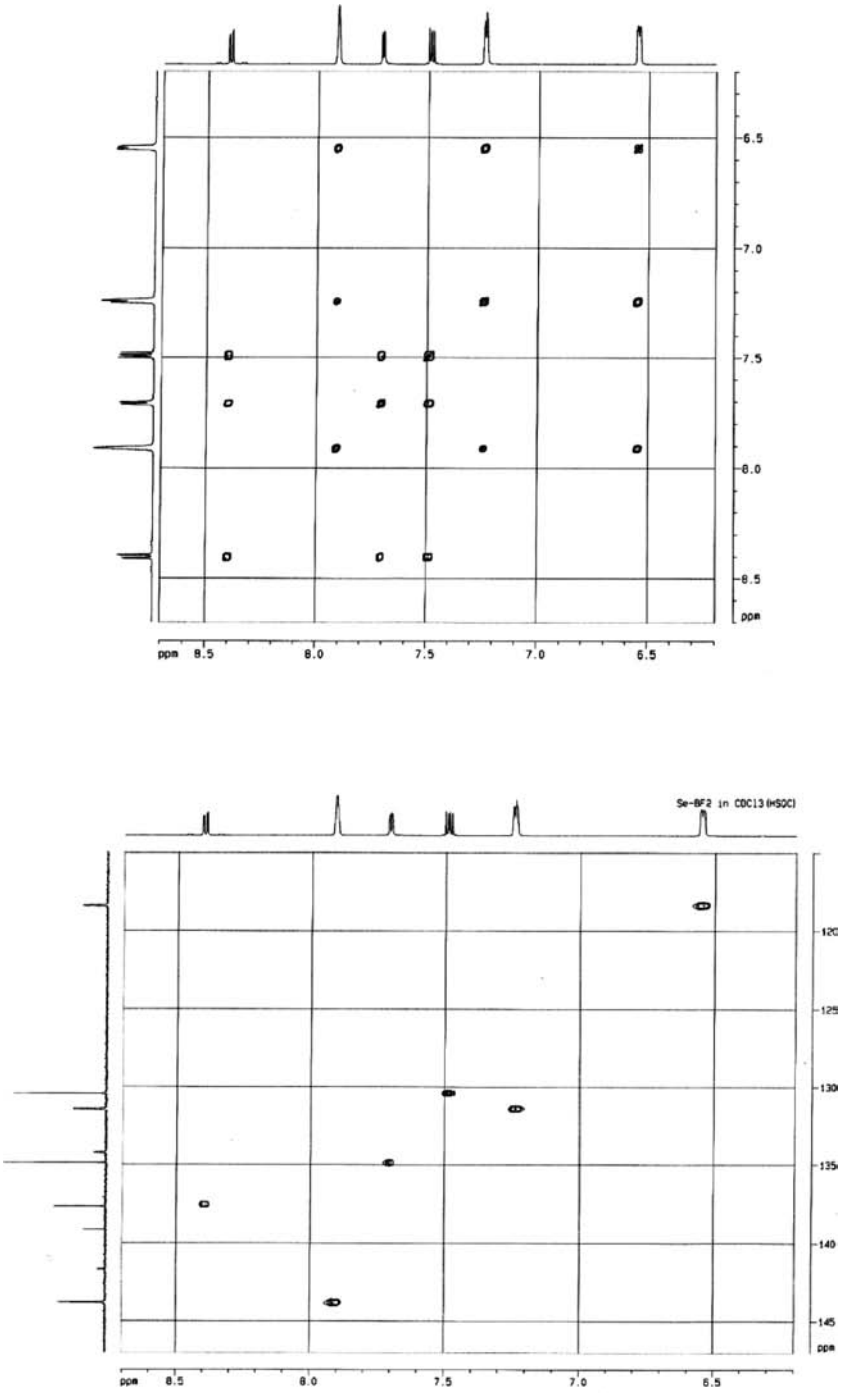

Figure 1. 2-D (^{1}H−^{1}H) COSY (*top*) and ^{1}H−^{13}C HSQC (*bottom*) NMR spectra for compound **9**.

and 2-D NMR (^{1}H−^{1}H COSY, ^{1}H−^{13}C HSQC and ^{1}H−^{13}C HMBC) spectra of compounds **7**, **9**, and **10** are shown in the Supporting Information. Further ^{11}B and ^{19}F NMR spectra were acquired as well (vide infra). Importantly, 2D-NMR experiments such as ^{1}H−^{1}H COSY, ^{1}H−^{13}C HSQC, and ^{1}H−^{13}C HMBC allowed for great clarity in atom assignments. Two examples for compound **9**, the first BODIPY selenenyl, are provided below (Figure 1). Chemical shifts of hydrogen atoms in the pyrrole ring for all compounds are listed in Table 1. The numbering of atoms is based on those found in Scheme 1.

With respect to the three pairs of pyrrolyl protons, proton 1 is located adjacent to the nitrogen atom, proton 2 is the middle atom in pyrrolyl ring, whereas proton 3 is positioned closest to the rotating heterocyclic ring. Each proton for compounds **7**, **9**, and **10** has been carefully assigned herein using the ^{1}H NMR spectrum in $CDCl_3$. By inspection of chemical shifts, it appears that proton 1 is more deshielded than the other protons, based on its proximity to an electron-rich heteroatom.

Table 1. Chemical Shifts (ppm) of Selected Protons in Compounds **7**−**11** (in $CDCl_3$)

proton	**7**	**8**	**9**	**10**	**11**
1	7.86	7.91	7.91	7.89	7.90
2	6.55	6.56	6.55	6.54	6.54
3	7.44	7.26	7.24	7.18	7.09

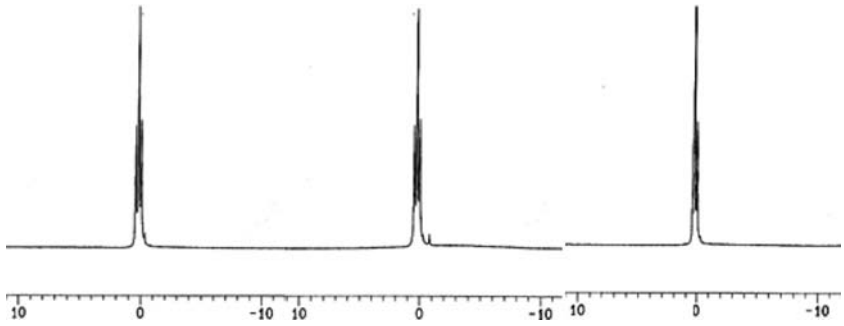

Figure 2. ^{11}B-NMR spectra of **7** (δ 0.20, $^1J_{B-F}$ = 28.5 Hz), **9** (δ 0.23, $^1J_{B-F}$ = 28.6 Hz), and **10** (δ 0.24, $^1J_{B-F}$ = 28.7 Hz) in $CDCl_3$.

In these 2-substituted compounds (**7**−**9**), the chemical shifts of protons 1 and 2 are similar, but there is a ~0.2 ppm difference for proton 3 which is, again, closest to the differentiated aryl ring. Proton 3 in compound **7** is more deshielded than that for **8** and **9**. Further, in the crystal structure, the dihedral angle between 8-position substitution ring and BODIPY core is obtained. Note that the angle in compound **7** is ~15° less than that of **8** or **9** (Table 4). This deshielding effect invokes the question of spacing: organic groups including π-bonds affect magnetic shielding or deshielding effects through space.[59] A lower static dihedral angle suggests a through-space closeness between the proton and the heteroatom (O, S, Se) in the conjugated ring. For compound **7**, because proton 3 is close to the oxygen atom, a more electron rich environment is formed here than would be expected for **8** and **9**. This consideration can be also extended to compounds **9** and **10**. A dihedral angle difference of 5.5° is accompanied by a chemical shift that is formally shifted δ 0.09 ppm downfield. Also, the chemical shift of proton 3 for compounds **7**−**9** (δ 7.24−7.44) is located more downfield than those of **10**−**11** (δ 7.09−7.18). The difference in location of heteroatom at the 2- or 3-position in the heterocyclic ring is also manifested in NMR signal protons.

Other nuclei can also be probed. ^{11}B NMR spectra were also acquired and revealed 1:2:1 triplet peaks from $^1J_{B-F}$ coupling with the adjacent fluorine atoms signifying the presence of a *di*fluoroboryl [BF_2] unit (Figure 2). The δ and coupling constant assignments in the ^{11}B NMR spectra (28.7 Hz for **8**, 28.4 Hz for **11**) are quite similar to the thienyl-substituted BODIPY compounds previously reported by our group[37a] and will not be discussed further. Interestingly, we can see the influence of the difluoro moiety for the C_1 atoms in a through-bond coupling (**7** and **9**: $^3J_{C-F}$ = 9.0 Hz; **10**: $^3J_{C-F}$ = 8.8 Hz) giving a doublet of triplets. Fluorine NMR spectra were also obtained for completeness and are summarized below in Table 2.

MALDI-TOF mass spectrometry was also undertaken to confirm solubility integrity. These showed the existence of the target compounds and, in some cases, the base-peak was positioned at the corresponding molecular weight assigned to a BODIPY unit formulation minus one fluorine atom.

Structural Comparison. The molecular structures of compounds **7**, **9**, and **10** have been determined by single crystal X-ray diffraction (Figure 3). Data collection was undertaken at 298 K for compound **7** and 100 K for compounds **9** and **10**. Both furyl-substituted BODIPY compounds, **7** and **10**, crystallize in the monoclinic crystal system, but were crystallographically determined to abide by the different space groups, *Cc* and $P2_1/c$, respectively. The selenenyl-substituted compound **9** crystallizes in the orthorhombic space group $P2_12_12_1$. From the literature, the 3-thienyl-substituted compound **11** exists in the monoclinic *Cc* space group; compound **8** appears in the orthorhombic $P2_12_12_1$ space group.[36,37a] Some important features from this crystal data for compounds **7**−**11** are summarized in Table 3. Crystal structure refinement data and selected bond length and angles are shown in the Supporting Information.

Table 2. ^{19}F-NMR Spectroscopic Data for Compounds **7**−**11**

compound	**7**	**8**	**9**	**10**	**11**
chemical shift (δ)	146.26	145.79	145.78	145.89	145.77
coupling constants (J_{B-F}, Hz)	28.5	28.5	28.8	28.8	28.8

In Table 3, we provide a comparison of some crystallographic features based on the subtle differences that arise through formal change of the aryl ring at the 8-position. In compounds **7**−**9**, when going down Group 16, a change from oxygen to selenium predictably makes that unit cell volume (V)-to-unit number (Z) ratio and calculated density increase; sulfur being of intermediate size and weight between Se and O, exhibits an intermediate value (294.8 Å^3/molecule). These trends in molecular densities are present despite comparing different cell systems (monoclinic versus orthorhombic). In compounds **10** and **11**, the V/Z value was inspected and found to also increase with the change from oxygen to sulfur. The calculated density for compound **11**, however, is marginally smaller than that found for compound **10**.

The BODIPY core mean plane (mean planes 1 + 3), which includes atoms C1−C9, N1, N2, and B1 is often casually considered rigid, and mistakenly thought of as planar; in almost all cases, there is a degree of inherent puckering as reflected by the depiction in Figure 3. Herein, there are some measurable distortions principally because of a function of 8-position substitution. First, the deviations in mean plane 1 (and including boron) for **7**−**9** have been calculated: 0.040 for **7**, 0.119 for **8**, and 0.123 for **9**. This also shows a trend with increasing atomic number for the group 16 element. Many 8-position substituted rings (plane 2, Figure 3) are rotated toward the main dipyrrin framework mean plane (plane 1). Also, two pyrrolyl planes (4 and 5) are slightly distorted: the boron atom is slightly puckered from the main dipyrrin framework (plane 1).

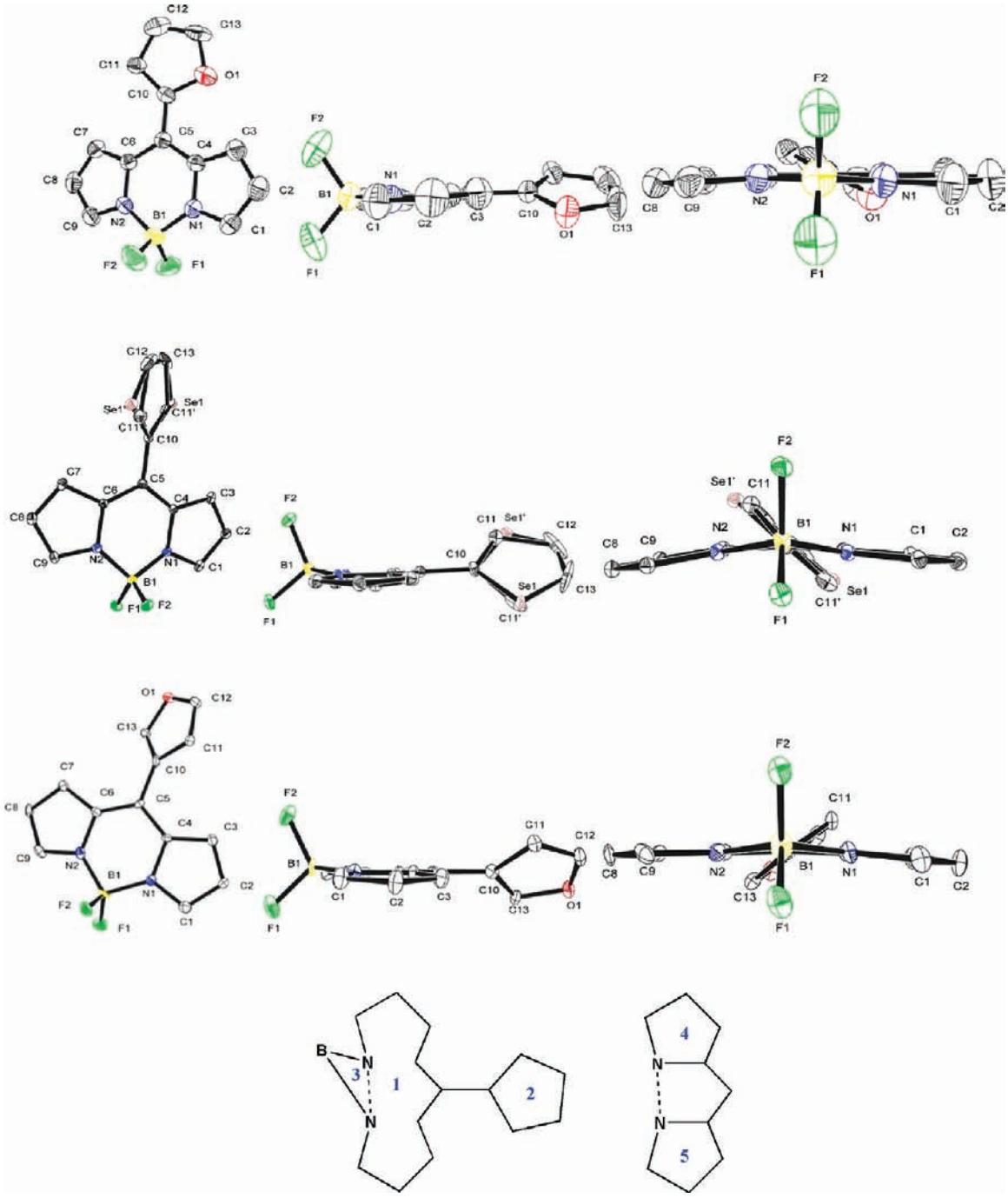

Figure 3. Top, side, and front views of the crystallographic molecular structures of compounds **7**, **9**, and **10**. Thermal ellipsoids are drawn at 30% probability level. Hydrogen atoms are omitted for clarity. (*Bottom*) Selected mean planes for the 8-aryl BODIPY framework discussed herein.

Table 3. Notable Crystallographic Features for Compounds **7**−**11**

	compound # (common descriptor)				
	7 (**"2-O"**)	**8** (**"2-S"**)	**9** (**"2-Se"**)	**10** (**"3-O"**)	**11** (**"3-S"**)
crystal system	monoclinic	orthorhombic	orthorhombic	monoclinic	monoclinic
space group	$P2_1/c$	$P2_12_12_1$	$P2_12_12_1$	Cc	Cc
V (Å^3)	2346.9(18)	1179.0(17)	1192.69(3)	1141.10(17)	1227.27(14)
Z	8	4	4	4	4
V/Z (Å^3/molecule)	293.4	294.8	298.2	285.3	306.8
P_{calcd} (g/cm^3)	1.461	1.544	1.788	1.502	1.483

Dihedral angles between selected planes are calculated using all non-hydrogen atoms through convenient use of the XP graphics interface from the SHELXL program.[46] These results are summarized in Table 4. All other related dihedral angles have been determined for compounds **7**, **9**, and **10** and are provided in the Supporting Information.

Table 4. Selected Dihedral Angles (deg) in Compounds **7**−**11**

mean planes	**7**	**8**	**9**	**10**	**11**
1 − 2 (deg)	26.6	42.4	43.7	38.7	44.2
1 − 3 (deg)	5.0	16.1	16.1	9.2	8.2
4 − 5 (deg)	4.9	14.3	14.7	6.8	7.0

Most of these compounds have a dihedral angle of ∼40° between planes 1 and 2. These results are reasonable in considering a sterically unhindered ring; but, larger angles are expected for the hindered ring substituents such as mesityl (∼75°) or *o*-tolyl (∼85°) enforcing a restricted ring motion between the pyrrolyl sides and the aryl ortho methyls.[5,35] Separately, BODIPY substitution could influence this as well. This dihedral angle for the 2-selenenyl-containing compound **9** is ∼43.7°, larger than that for the 2-furyl-substituted compound **7** (∼26.6°). The 2-thienyl-substituted compound **8** has an intermediate value (∼42.4°), but is closer to that for **9**;[37a] so, the heavy atom-containing ring is positioned in a more rotated orientation toward the extreme of 90°, explained simply on grounds of steric hindrance. Angles closer to the other extreme of 0° would be favored by "smaller" aryl groups and would promote greater π-electron density delocalization, and thus enhanced optical characteristics. While this static conformation is unmanageable for the *o*-tolyl or mesityl groups, it *can* be accomplished, with some ease, for the phenyl case; but ultimately this static structure deforms plane 1 and leads to fluorophore nonradiative deexcitation.[5] Crystallographically, compound **10** has a 38.7° dihedral angle between planes 1 and 2, larger than that in compound **7**.

A substituent *positional* difference (2- versus 3-furyl) is also interesting to consider: this formal change gives a 12° increase in the dihedral angles between mean planes 1 and 2 in the solid state. In compound **7**, the interaction between oxygen atoms and proximal hydrogen atoms (H3 in Scheme 1) may be able to stabilize the structure with a relatively small dihedral angle. The structures of compounds **8** and **9** are slightly more distorted than that for compound **7**.

We can now look at other dihedral angles such as the one between mean planes 1 and 3. This dihedral angle for both **8** and **9** is ∼16.1°, whereas that for **7** is tending toward planar at ∼5.0°. Also, the angle between mean planes 4 and 5 is ∼14.7° for **9**; it is ∼14.3° for compound **8** and ∼4.9° for compound **7**. The puckering of the boron atom away from plane 1 gives rise to the disorder of the 8-position substituted ring and thus two possible "*syn*" and "*anti*" type conformers.[37a] The crystal structures for the thienyl- and selenenyl-substituted compounds **8** and **9** showed the existence of two conformers by way of crystallographic disorder (Figure 3);[37a] but solution studies for the furyl-substituted compounds **7** and **10** have not revealed the same dramatic disordering on the NMR time scale (RT). In compound **7**, the bond lengths for N(1)−C(1) and N(2)−C(9) [1.337(4) Å for both] are slightly, yet discernibly, larger than those of N(1)−C(4) and N(2)−C(6) [1.393(4) and 1.385(4) Å, respectively], which suggests that the former bonds are *localized* double bonds.[35] This has implications in our depicting the BODIPY core with discretely localized π-bonding instead of with universally delocalized bonding. The other compounds (**8** and **10**) have also same bond length alternation as seen structurally. This alternating double bond character is a special feature of the BODIPY structure.

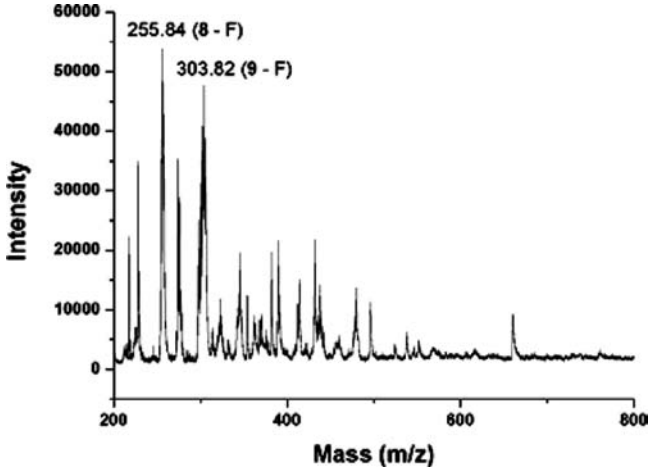

Figure 4. MALDI-TOF spectrum showing evidence for the co-crystallization of **8** and **9**.

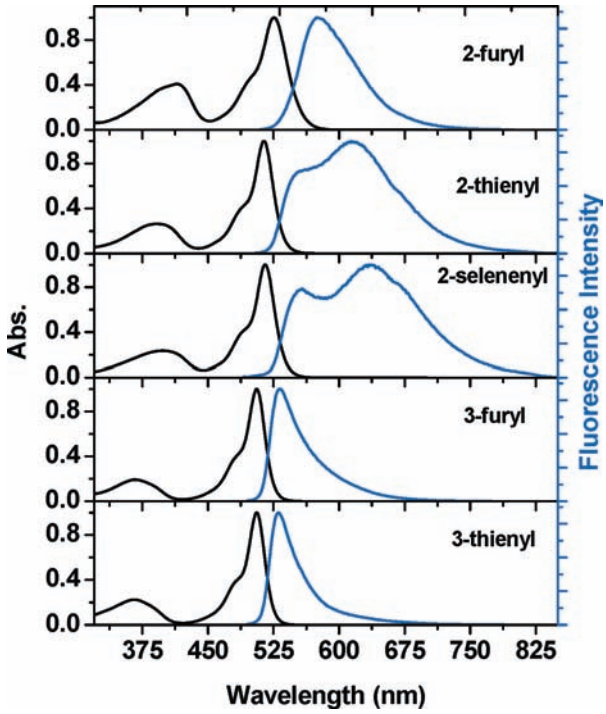

Figure 5. Comparative normalized absorption and emission spectra of **7**−**11** in toluene 5.0×10^{-6} M.

Co-crystallization of Compounds 8 and 9. The same crystal system and space group for compounds **8** and **9** give the possibility for co-crystallization. Both compounds are found to form crystals in the orthorhombic space group $P2_12_12_1$. A 1:1 mixture of **8** and **9** from a dichloromethane/hexane solvent was used to try to effect such "doping." Red crystals were discovered to have formed after 2 days; one was chosen for mass spectrometric analysis which appeared to be single (not *twinned*), to the limit of the authors' visual acuity, under a laboratory microscope. A MALDI-TOF spectrum shows the coexistence of two main peaks in a ∼ 6:5 ratio (Figure 4) that correspond well to the calculated molecular weight of compounds **8** ($[M\text{-}F]^+$ = 255.06)

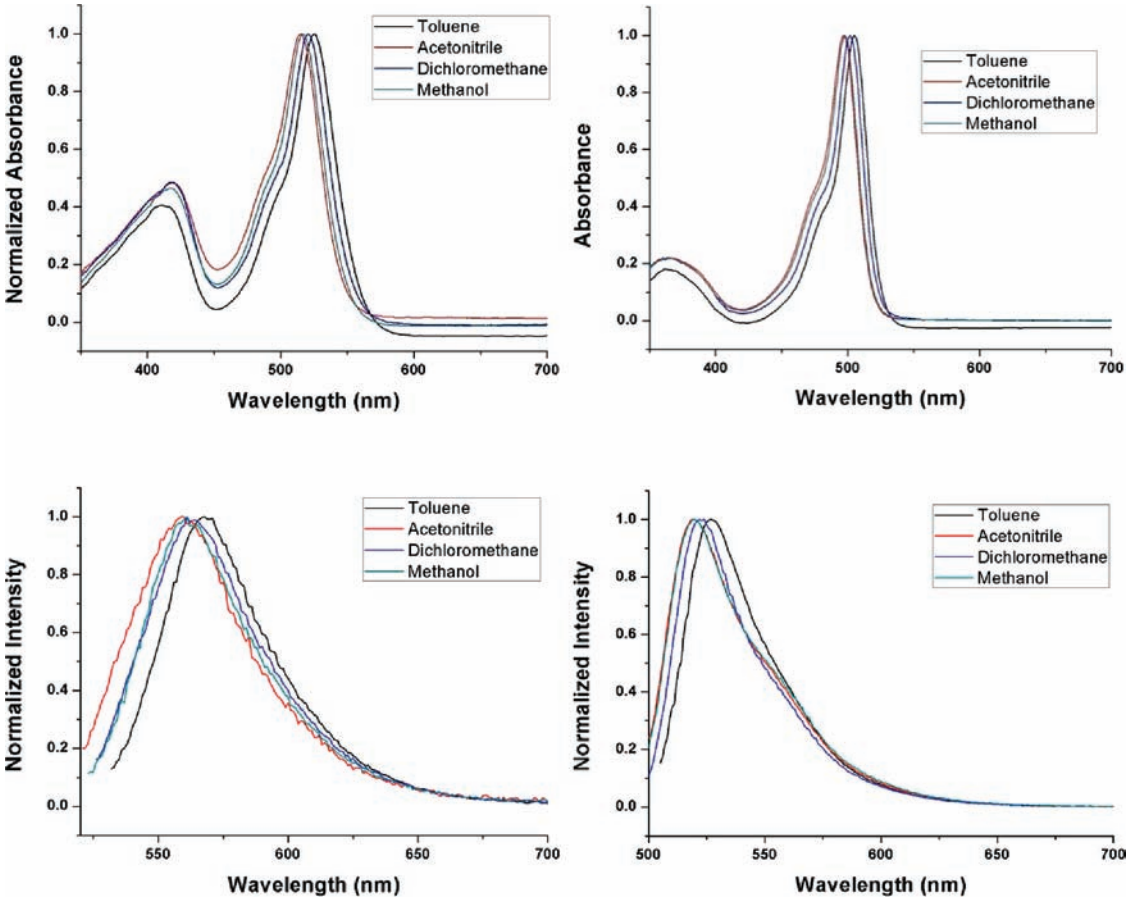

Figure 6. Normalized absorption spectra of **7** (*top left*) and **10** (*top right*) and emission spectra of **7** (*bottom left*) and **10** (*bottom right*) (5.0×10^{-6} M) in several solvents.

and **9** ([M-F]$^+$ = 303.01), signifying the successful co-crystallization of **8** and **9**.

Absorption and Emission Spectra. UV−vis absorbance and emission spectra were acquired for the novel compounds reported herein in acetonitrile, dichloromethane, methanol, and toluene (Figure 6). Key values of this photophysical data for compounds **7**−**11** have been compiled in Table 5.

In the absorption spectrum, a strong absorbance band with an absorption coefficient in the order of 30,000−60,000 M^{-1} cm^{-1} appears at about 500 nm and is assigned to the S_0-S_1 transition. In the wavelength region below the absorption maximum, there exists a "shoulder" at about 480 nm assigned to the 0−1 vibrational transition. Finally, a second and higher energy absorption maximum peak is shown broadly at ∼370−400 nm assigned to the S_0-S_2 transition. These three peaks constitute the main optical features of the BODIPY system absorption spectrum[51] and are revealed in the spectra for compounds **7**−**11**. Red (bathochromic) shifting usually occurs in relatively nonpolar solvents such as toluene, compared to when the BODIPY is in polar solvents such as acetonitrile (Figure 6 and Supporting Information): **7** (10 nm), **8** (8 nm), **9** (9 nm), **10** (8 nm), and **11** (8 nm). This hypsochromic shifting under nonpolar conditions is common for BODIPY[52−54] and cyanine systems.[55] The 2-heterocyclically substituted compounds (**7**−**9**) have absorption maxima at higher wavelengths (515, 505, and 506 nm, respectively) than for those of the 3-heterocyclically substituted compounds **10**−**11** (497 nm for both) in, for example, acetonitrile. The electron-withdrawing effect for the 2-heterocycle would be expected to be larger than that for the 3-heterocycle. For further analysis, the Hammett substituent constant (σ_m or σ_3) of 0.06 for 2-furyl, 0.09 for 2-thienyl, 0.03 for 3-thienyl, and 0.06 for 2-selenenyl can be invoked.[56] The electron withdrawing effect of the 8-position substituent would delocalize the electron density of the LUMO level; thus, the LUMO level can be energetically stabilized. There is presumed to be little energy change in the HOMO because it has a node at the 8-position (See the computational Results and Discussion below). Therefore, the energy gap between the HOMO and LUMO energy levels would be decreased leading to a greater value for $\lambda_{abs,max}$.

(51) Qin, W. W.; Baruah, M.; Van der Auweraer, M.; De Schryver, F. C.; Boens, N. *J. Phys. Chem. A* **2005**, *109*, 7371.
(52) Kollmannsberger, M. R.; Resch-Genger, U.; Daub, J. *J. Phys. Chem. A* **1998**, *102*, 10211.
(53) Banuelos Prieto, J.; Lopez Arbeloa, F.; Martínez Martínez, V.; Arbeloa Lopez, T.; Liras, M.; Lopez Arbeloa, I. *Chem. Phys. Lett.* **2004**, *385*, 29.
(54) Costela, A.; García-Moreno, I.; Gómez, C.; Sastre, R.; Amat-Guerri, F.; Liras, M.; Lopez Arbeloa, F.; Banuelos Prieto, J.; Lopez Arbeloa, I. *J. Phys. Chem. A* **2002**, *106*, 7736.
(55) Noukakis, D.; Van der Auweraer, M.; De Schryver, F. C. *J. Phys. Chem. A* **1995**, *99*, 11860.
(56) Hansch, C.; Leo, A.; Taft, R. W. *Chem. Rev.* **1991**, *91*, 165.

Respective emission spectra also show a similar trend with those for the absorption spectra. Specifically, a fluorescence emission is detected at ~560 nm for compound **7** and ~520 nm for compounds **10** and **11**. Compounds **8** and **9** show very little emission intensity. Fluorescence bands are *batho*chromically shifted with decreasing solvent polarity from acetonitrile to toluene (Figure 6). Also, Φ_F decreases with increasing solvent polarity, similar to what has previously been reported in the BODIPY literature, because of an increase in the nonradiative rate constant.[51] The 2-furyl-substituted species (**7**) bears a Stokes shift (~40 nm) almost twice larger than those for **10** and **11** (~20 nm); in the excited state for compound **7**, it is likely that a greater degree of geometrical flexibility allows for an increasing incidence of nonradiative decay.[51] In photographs of solutions for the dissolved compounds (Figure 7), the solutions of the 2-heterocyclically substituted species (**7**−**9**) are clearly red, and those for **10** and **11** are orange, respectively. Under UV light (benchtop lamp, $\lambda_{excitation}$ = 365 nm), solutions of **7**, **10**, and **11** exhibit quite strong fluorescence, whereas **8** and **9** do not.

Table 5. Select Photophysical Data for Novel Compounds and Related Literature Compounds (**7**−**11**)

BODIPY solvent	$\lambda_{abs,max}$ (nm)	absorption coefficient (ε, M^{-1} cm^{-1})	$\lambda_{em,max}$ (nm)	Stokes shift (nm)	fluorescence quantum yield (Φ_F)
compound **7**					
CH_3CN	515	$(3.4 \pm 0.09) \times 10^4$	559	44	0.018
CH_2Cl_2	520	$(3.8 \pm 0.06) \times 10^4$	561	41	0.039
MeOH	516	$(4.0 \pm 0.06) \times 10^4$	561	45	0.024
toluene	525	$(4.2 \pm 0.07) \times 10^4$	568	43	0.055
compound **8**					
CH_3CN	505	$(4.6 \pm 0.04) \times 10^4$			0.0025
CH_2Cl_2	510	$(5.4 \pm 0.25) \times 10^4$			0.0047
MeOH	506	$(5.0 \pm 0.09) \times 10^4$			0.0031
toluene	513	$(5.4 \pm 0.07) \times 10^4$			0.0077
compound **9**					
CH_3CN	506	$(4.3 \pm 0.10) \times 10^4$			0.0015
CH_2Cl_2	511	$(5.2 \pm 0.17) \times 10^4$			0.0015
MeOH	507	$(5.0 \pm 0.10) \times 10^4$			0.0012
toluene	515	$(5.6 \pm 0.08) \times 10^4$			0.0027
compound **10**					
CH_3CN	497	$(4.7 \pm 0.06) \times 10^4$	519	22	0.11
CH_2Cl_2	502	$(5.8 \pm 0.23) \times 10^4$	524	22	0.16
MeOH	498	$(5.4 \pm 0.08) \times 10^4$	519	21	0.11
toluene	505	$(5.6 \pm 0.10) \times 10^4$	527	22	0.24
compound **11**					
CH_3CN	497	$(5.20 \pm 0.04) \times 10^4$	519	22	0.025
CH_2Cl_2	502	$(6.0 \pm 0.17) \times 10^4$	522	20	0.059
MeOH	498	$(5.7 \pm 0.09) \times 10^4$	518	20	0.033
toluene	505	$(6.6 \pm 0.09) \times 10^4$	526	21	0.096

It is convenient to compare absorptive and emissive characteristics for all five derivatives together (Figure 8) in a stacked arrangement from a single solvent. BODIPY derivatives show intense absorption at 526, 514, 514, 506, and 506 nm, respectively, for the **7, 8, 9, 10,** and **11** in toluene. These spectral changes reveal a strong electronic interaction between the substituent and BODIPY moiety. Similarly, the fluorescence spectra measured in toluene correspond to 574, 560 (614), 557 (636), 533, and 530 nm for the **7, 8, 9, 10,** and **11**, respectively. Among these, only **10** and **11** exhibit mirror image relationship with the absorption spectra, a characteristic behavior generally observed for BODIPY derivatives. **8** and **9** derivatives show two well-resolved fluorescence peaks, which, however, have no "mirror image" relationship with their absorption spectra. But, the **7** shows only one fluorescence peak; its fwhm (full-width at half-maximum) is comparatively larger (ca. 2116 cm^{-1}) than that of **10** (ca. 1469 cm^{-1}) derivative. Notably, the lower-energy fluorescence peak becomes intense while going from furyl to selenenyl, that is, while decreasing the electronegativity of the heteroatom. The appearance of two-fluorescence peaks is quite unusual for BODIPY derivatives; however, the 8-*p*-aminophenyl derivative shows *two* fluorescence bands corresponding to the emission from (*i*) the local excited state and (*ii*) a charge transfer (CT) state, in which only the latter is sensitive to solvent polarity.[51] We have not carried out extensive solvent-dependent fluorescence studies for these molecules, but the results here and from our previous report[37a] suggests that the fluorescence spectra of **8** seems to be relatively insensitive to the

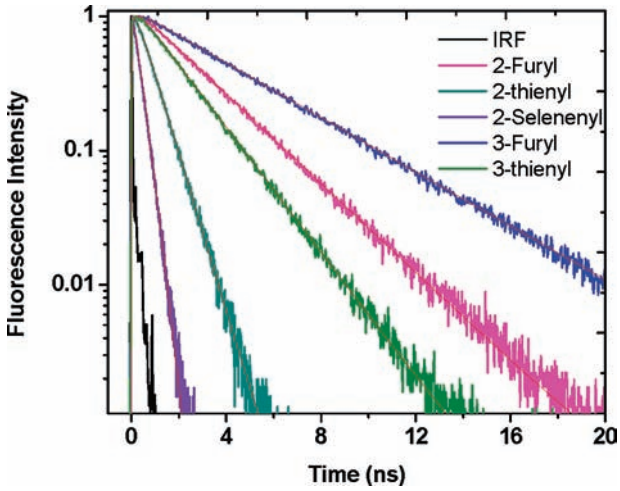

Figure 8. Fluorescence decay for compounds **7**−**11**. IRF = instrumental response function.

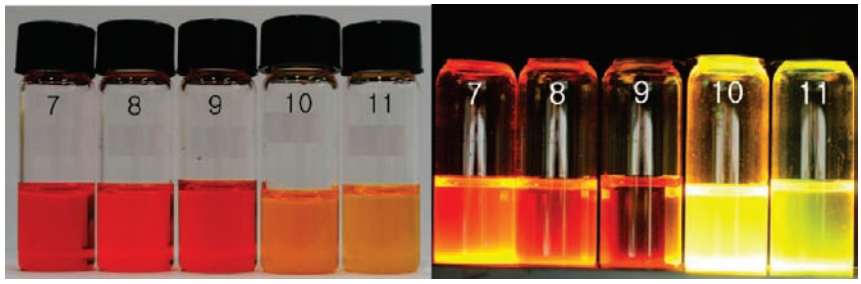

Figure 7. Solutions of compounds **7**−**11** (1.0×10^{-3} M) in toluene under (*left*) normal light and (*right*) UV light ($\lambda_{excitation}$ = 365 nm).

Table 6. Photophysical Properties of Compounds **7**−**11** in Toluene

compound	lifetime (ns)	K_r (10^7 s^{-1})	K_{nr} (10^8 s^{-1})
7	2.60	2.12	3.63
8	0.74		
9	0.27		
10	4.26	5.63	1.78
11	1.86	5.16	4.86

solvent polarity. Thus, the origin of the dual fluorescence is not clear at this moment. It may be due to a different conformer for the excited state, or from a CT state (*sensitivity to the nature of heteroatom*). More systematic studies are needed to understand this phenomenon.

Photophysics. The photophysical properties of BODIPY dyes with different *meso*- substituents, namely, 2-furyl, 2-thienyl, 2-selenenyl, 3-furyl, and 3-thienyl, were carried out in toluene. The fluorescence quantum yields for derivatives **7**−**11** are comparatively smaller than that of the *meso*-phenyl substituent (Φ_F = 0.42) because of the electron donation effects of the heteroatom to the BODIPY moiety (Table 5). This interpretation is consistent with the decrease in Φ_F as the electronegativity of the heteroatom decreases. Furthermore, the fluorescence lifetimes of BODIPY derivatives measured by the TCSPC technique ($\lambda_{excitation}$ = 460 nm) also show a similar trend. The fluorescence lifetimes were measured to be 2.60, 0.74, 0.27, 4.26, and 1.86 ns, respectively, for the **7**, **8**, **9**, **10**, and **11** derivatives (Figure 8). We have also calculated the radiative ($k_r = \Phi_F/\tau_F$) and nonradiative ($k_{nr} = (1 - \Phi_F)/\tau_F$) rate constants using Φ_F and fluorescence lifetime values (Table 6). In the case of the **10** and **11** derivatives, the radiative rate constants are similar, whereas the *non*radiative rate constant for **11** is nearly ~2.5 times larger than that of **10**. Thus, it can be concluded that a systematic diminishment of BODIPY fluorescence properties with decreasing electronegativity of the heteroatom can be attributed to electron donating ability.

Significant changes in the photophysical properties were observed when the 8-heterocyclic attachment was formally changed from the 2- to 3- position. Namely, the absorption and fluorescence spectra of the BODIPY species are comparatively blue-shifted when the heteroatom is formally moved from 2- to the 3- position. This feature suggests that the electronic interaction between the *meso*-substituent and BODIPY moiety is stronger when the heteroatom is at the 2-position. This behavior is understandable in the sense that free *meso* substituent rotation is facilitated with a 2-heterocycle; the 3-heterocycle introduces additional steric interaction between the CH hydrogen at the 2-position and BODIPY moiety, thus reducing the electronic interaction. The larger Stokes shifts observed for the **7** and **8** compared to those of their 3-heteroatom substituted counterparts are also consistent with the occurrence of larger geometric rearrangements upon photoexcitation for the former. Another possibility for this behavior relates to the electron donating ability of the heteratom, likened to the *ortho*, *meta*, and *para* effect for phenyl substition.

Emission wavelength-dependent decays were also considered in this study (Figure 9). The 2-thienyl substituted BODIPY system, **8**, shows emission wavelength dependent fluorescence decay. An instrument response limited short component and a long-lived species (ca. 0.74 ns)

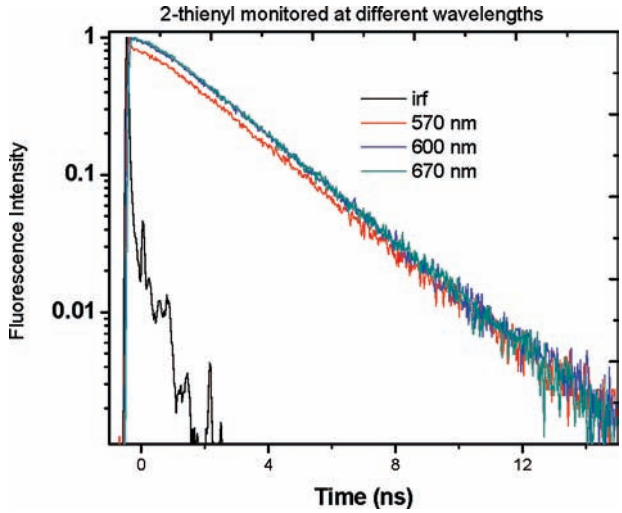

Figure 9. Emission wavelength-dependent decay for compound **8**. IRF + instrumental response function.

were observed at 570 nm. However, only the single-component with the lifetime of 0.74 ns was observed when the fluorescence was monitored at 600 and 670 nm. This experiment can later be repeated over a range of wavelengths and also at shorter time scales.

Computational Results. We undertook DFT calculations to determine the electronic HOMO−LUMO energy differences for all five existing compounds (**7**−**11**) to endeavor to better understand the underlying reasons for the optical differences. The input structures are readily adapted from the X-ray crystallographic coordinates, and a geometry optimization followed by a frequency analysis gave new structures that can give HOMO−LUMO energy level information. The structure of compound **8** has previously been minimized and has been recalculated herein. By inspection from the diagrams in Table 7, in the HOMO depictions, there is no electron density on the 8-position carbon in the BODIPY fluorophores, indicative of a node. This diagram could explain the phenomenon that red-shifting of absorption and emission spectra may be concomitant with the electron withdrawing group capability of the 8-position substituent. In compounds **7** and **10**, the furyl ring has no electron density in the LUMO, while the HOMO state has large electron density through their whole structure. The HOMO level for compound **9** and **11** is different with other compounds. Electron density is located in the selenenyl ring and almost no electron density at the BODIPY core. HOMO−LUMO energy gap is larger in **7**, **8** (48.3 kcal mol^{-1}, *recalculated*), **10**, and **11** than **9** (37.0 kcal mol^{-1}) by about ~10 kcal mol^{-1}. These gas phase calculations all provide a basic separation in electron clouds for the HOMO−LUMO orbitals; however, there are some important discrepancies between these computational and our optical results. The electronic distribution in the HOMO state of compounds **9** and **11** are mainly delocalized in the 8-aryl substituent rather than in the BODIPY core, but this is not true for their LUMO state (Table 7). The electronic distribution in the HOMO and LUMO states of compounds **7** and **10** are mainly delocalized in the BODIPY ring. Consequently, important changes in the absorption and fluorescence spectra of

Table 7. HOMO-LUMO Diagrams from Theoretically Geometry Optimized Structures of Compounds **7**, **9**, **10**, and **11** with Energies in kcal mol^{-1}.

Compound	HOMO	LUMO
7	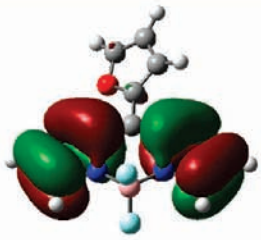	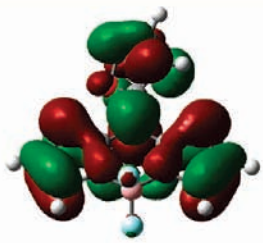
Energy (Hartrees)	-0.325	-0.249
ΔE (kcal mol^{-1})	47.7	
9	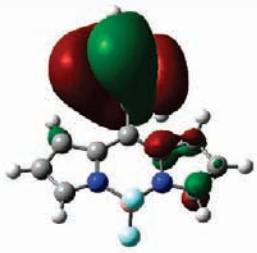	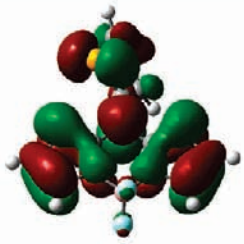
Energy (Hartrees)	-0.305	-0.246
ΔE (kcal mol^{-1})	37.0	
10	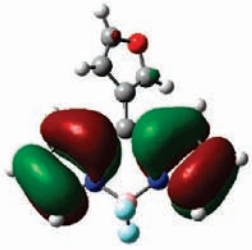	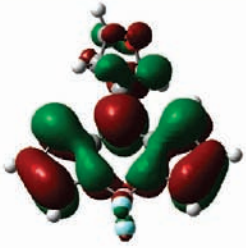
Energy (Hartrees)	-0.325	-0.246
ΔE (kcal mol^{-1})	49.6	
11	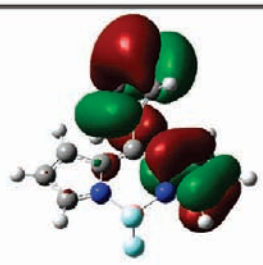	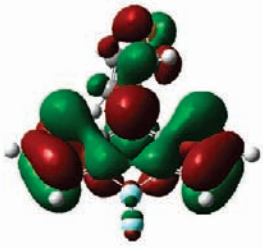
Energy (Hartrees)	-0.324	-0.246
ΔE (kcal mol^{-1})	49.0	

compounds **9** and **11** with respect to those of compounds **7** and **10** should be expected. Also, the theoretical *E* value of compound **9** (37 kcal/mol) is much lower than for those of other compounds (around 48 kcal/mol), and a large Stokes shift should be expected for **9** and **11**. Thus, these differences/anomalies may arise from the limitations of extending the results acquired for theory performed in the gas phase to solution systems. Further DFT studies can be undertaken to better understand possible solution-gas phase differences.

Reactivity with Hydrogen Peroxide and Molecular Bromine. Furyl-substituted BODIPY compounds **7** and **10** were titrated with hydrogen peroxide: but there is no absorbance change, even under the addition of a great excess of H_2O_2 and at extended times (45+ h) (Supporting Information). Also there is no intensity change in the emission spectra with increasing amount of H_2O_2 (up to 500 equiv). This indicates that there is no facile BODIPY decomposition. Interestingly, the same inertness is also seen for compounds **8**, **9**, and **11** (see Supporting

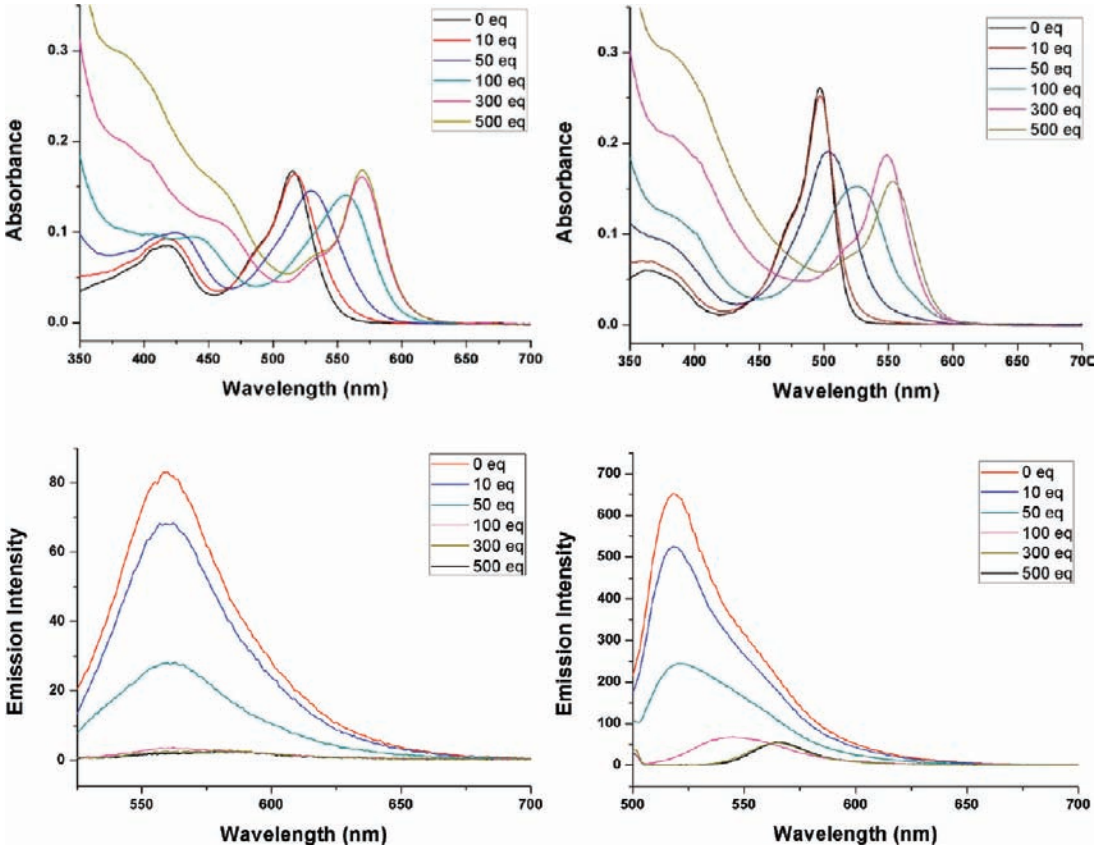

Figure 10. Absorbance spectra of a titration of Br_2 with compounds **7** (*top left*) and **10** (*top right*) in acetonitrile after 10 h. Emission spectra of titration of Br_2 with compound **7** (*bottom left*) and **10** (*bottom right*) in acetonitrile after 2 h. Dye concentration is 5×10^{-6} M.

Information) in light of the fact that a sulfone species can be prepared for a related system through the use of *m*-CPBA.[36] This suggests that these systems have an enhanced resistance to peroxide media, and future related species stand as definite possibilities for continued use in physiological systems such as in studying brain chemistry.[57,58]

Also, BODIPY fluorophore bromination was effected. A titration of the BODIPY compounds (**7**, **9**, and **10**) with molecular bromine (Br_2) gives way to an even, progressive bathochromic shift of the $\lambda_{abs,max}$ band (~500 nm → ~560 nm) observed with additions of up to a large excess (i.e., ≤ ~500 equiv). In the emission spectra, the intensity decreases with increasing amount of bromine and a bathochromic shift ensues. There appears to be definite and even product formation, in the absence of decomposition (Figure 10 and Supporting Information). This result is in line with previous results of related systems[36] and is reasonable when considering the likely stepwise bromine substitution at the pyrrolic and furyl-/thienyl-/seleneyl-ring positions: the electron density in the BODIPY core is delocalized and energetically stabilized. Thus, the titration with molecular bromine reveals a continuum of novel brominated BODIPY fluorophore products for **7**, **9**, and **10** which have yet to be isolated and fully characterized. Also, we reported that the reactions between BODIPY fluorophore and molecular bromine give tetra- and hexabrominated BODIPY derivatives that can be isolated via step-by-step substitution.[36] Importantly, this also underscores the resilience of these BODIPY systems when exposed to a different oxidant.

4. Conclusion

In this report, we have described a variety of new results for novel, interesting, and potentially practical fluorescent BODIPY species. We have synthesized three novel BODIPY molecules herein. These have been fully characterized by techniques, including single-crystal X-ray diffraction, and 2-D NMR spectroscopy. These derivatives constitute a growing class of 5-membered 8-aryl BODIPY species. The close relationship between derivatives allows for some interesting structural (solid) and optical (solution) comparisons that stem from our previous work with 8-thienyl-substituted derivatives. Crystallographically, depending on the 8-position substitution (one-chalcogen atom differences), compounds have different crystal systems and space groups (monoclinic and orthorhombic; *Cc* (**10**), $P2_12_12_1$ (**9**), $P2_1/c$ (**7**)). A consideration of the same crystal system/space group for two different compounds led to the discovery that co-crystallization is possible for compounds **8** and **9**. Dihedral angles obtained from the structural studies between the heterocyclic ring and BODIPY core can be compared: that for **7** is smaller than those for **8** and **9**. To summarize, the distinct spectral properties of BODIPY with respect to the different substituents. Compounds **7**−**11** show strong characteristic absorbances ~500 and ~420 nm, along with shoulder peaks (~480 nm), characteristic of BODIPY species. Higher wavelengths of λ_{max} are represented with

(57) Mattson, M. P.; Lovell, M. A.; Furukawa, K.; Markesbery, W. R. *J. Neurochem.* **1995**, *65*, 1740.
(58) Halliwell, B. *J. Neurochem.* **1992**, *59*, 1609.
(59) Martin, N. H.; Brown., J. D.; Nance, K. H.; Schaefer, H. F.; Schleyer, P. V.; Wang, Z. X.; Woodcock, H. L. *Org. Lett.* **2001**, *3*, 3823.

decreasing solvent polarity in absorption and emission spectra. Compounds **7**−**9** show higher $\lambda_{abs,max}$ than **10** and **11** because of strong electron withdrawing effects imparted by the 2-heteroatom ring which may stabilize the LUMO state. The heteroatom position dependent properties are ascribed to the facile rotation of *meso*- substituent and/or the difference in the electron donating ability of 2- and 3- positions. The definite origin of dual emission is not yet clear. Fluorescence lifetimes were found to be 2.60 (**7**), 0.74 (**8**), 0.27 (**9**), 4.26 (**10**), and 1.86 ns (**11**); $\lambda_{em,max}$ decay was studied for **8**. A limited number of oxidation reactions were also undertaken revealing that BODIPY molecules have heightened resistance to hydrogen peroxide; differently, they can be gradually substituted with bromine (atoms) upon the addition of excess Br_2 which gives continuous bathochromic $\lambda_{abs,max}$ shifting to ~580 nm. X-ray single crystal diffraction was obtained and can be related to solution studies as well for these closely related compounds. Geometrical changes for **7**−**11** are related to differences in certain NMR signals. Compounds which have a lower dihedral angle between substitution rings and the BODIPY core give downfield NMR spectroscopic signals, that is, for proton 3; it appears that a *through-space* distance is correlated with its chemical shift. The shorter the proton heteroatom distance is (based on chalogen identity), the more downfield the shifting is. This work can be expanded to new BODIPY-type system designs bearing subtle differences on the atomic level. Derivatives of these types of fluorescent dyes will be explored as experimental molecular sensors in the life sciences, and hopefully utilized in earnest in the realm of molecular neurodegeneration.

Acknowledgment. D.G.C. acknowledges support from NRF (National Research Foundation) of Korea (Grant 2009-0070330) and from the Korea Science and Engineering Foundation (KOSEF) (Grant R01-2008-000-12388-0). Also, this work was supported by the "R&E" (Research and Education) program sponsored by KOSEF hosted by the KSA (Korea Science Academy, Pusan); high school-level students Mr. Jung Hwan Park, Mr. Joo Hoon Lee, Mr. Seok Joon Seo, and Mr. Eui Taek Jeong from this school helped prepare some derivatives reported herein. The URP (Undergraduate Research Program) program by KAIST also allotted money. Professor Chang Seop Hong (Department of Chemistry, Korea University) facilitated the X-ray diffraction study of Compounds **7**, **9**, and **10**. MALDI-TOF analyses were obtained with the help of the KAIST research supporting team. Mr. Hack Soo Shin is gratefully acknowledged for acquiring various NMR spectra. Teresa Linstead (Cambridge, England) is thanked for her assistance in filing the crystallographic data (CCDC #'s 756065, 756066, and 756067). ^{19}F NMR spectroscopic data was obtained at the Korea Basic Science Institute (Ochang Center).

Supporting Information Available: Reproductions (scans) of 1-D ^{1}H, ^{13}C, and 2-D COSY, HSQC, HMBC NMR spectra of compounds; ^{11}B and ^{19}F NMR spectra; MALDI-TOF spectra; UV−vis absorption and emission spectra in various solvents; Figures of UV−vis and emission Titration spectra in which hydrogen peroxide and molecular bromine; Crystallographic data tables and all bond lengths and bond angles; Dihedral angles of selected BODIPY planes; CIF files for the 3 crystallographic determinations. This material is available free of charge via the Internet at http://pubs.acs.org. The CIF files were also deposited with the Cambridge Crystallographic Data center (CCDC), and CCDC codes 756065, 706066, and 706067 were allocated. These data are available without cost at www.ccdc.cam.ac.uk/conts/retrieving.html or from the CCDC, 12 Union Road, Cambridge CB2 IEZ, United Kingdom; fax: +44(0)1223−336033; e-mail: deposit@ccdc.cam.ac.kr.